ELSEVIER

Polymer 42 (2001) 8103–8111

polymer

www.elsevier.nl/locate/polymer

# MCM-41 catalytic pyrolysis of ethylene–vinyl acetate copolymers: kinetic model

A. Marcilla*, A. Gómez, J.A. Reyes-Labarta

*Dpto. Ingeniería Química, Universidad de Alicante, Apdo. 99, Alicante 03080, Spain*

Received 20 February 2001; accepted 8 April 2001

**Abstract**

Six samples of commercial ethylene–vinyl acetate (EVA) copolymers with different vinyl acetate (VA) contents have been pyrolyzed with and without an MCM-41 acid catalyst in a TG equipment at 10 and 40 K/min and inert atmosphere ($N_2$). The classical shift to higher temperatures has been observed for all processes involved when increasing the heating rate, being the peak corresponding to the VA domains more sensitive than that of the PE. Results obtained suggest that the catalytic pyrolysis of this copolymer can be considered as the combination of the pyrolysis of three fractions: the decomposition of the VA domains, that seem to be unaltered by the presence of the catalyst; the decomposition of the corresponding polyene residue after its evolution; the decomposition of the PE domains. Thus, the effect of the catalyst increases as the amount of VA decreases in the copolymer. A kinetic model has been applied simultaneously to runs performed at different heating rates and catalyst concentration allowing a good correlation of the weight loss data. 

*Keywords*: MCM-41 catalyst; Copolymers; Ethylene–vinyl acetate

## 1. Introduction

Ethylene–vinyl acetate (EVA) copolymers represent the largest volume segment of the ethylene copolymer market. The properties of EVA copolymers depend on their vinyl acetate (VA) contents and products ranging from 2 to 40% of VA are commercialised for different purposes [1]. The accumulation of enormous amounts of plastic waste produced all over the world has negative implications on the environment, and a restrictive environmental legislation has forced the economy into extensive recycling activities [2]. Therefore, recycling plays an essential role in developing a sustainable economy and must be considered in any plastic application.

The pyrolysis of organic materials has received renewed attention due to the possibility of converting these wastes into useful energetic products or into valuable chemicals (chemical or ternary recycling). Thermogravimetrical analysis (TGA) alone and combined with complementary techniques such as DSC, GC, FTIR and MS, has been widely used to study the pyrolysis of different materials. In the case of EVA copolymers, the papers of Verdú and Devesa [3], Washall and Wampler [4], McGrattan [5], Marcilla and Beltrán [6], Häußler et al. [7] and Marcilla et al. [8] are examples of the use of these techniques to study and quantify the VA content in these type of copolymers. Different kinetic models to explain the weight loss of polymer samples under thermal treatment were developed and applied by Munteanu and Turcu [9] and Marcilla and Beltrán [6].

The thermal decomposition of EVA copolymers can be considered as a two-step process. First, acetic acid is evolved from the acetate, followed by the second step which corresponds to the main chain degradation. Munteanu and Turcu [10] suggested a mechanism for the first step of EVA copolymers decomposition. According to these authors, in the grafted chains, the decomposition of the acetoxy groups is favoured by the tendency to form (via hydrogen bonds with active methylene groups) a six-ring transition state. The activated complex decomposes thermally, eliminating acetic acid. The double bonds formed in the grafted chains have a '*trans*' configuration at the end of the decomposition that favours cross-linking. Moskala and Lee [11] pointed out that the acetic acid evolved may react with other polymer chains accelerating the weight loss. According to McGrattan [5], at around 640 K, acetate pyrolysis occurs, leaving a polyunsaturated linear hydrocarbon. A competing reaction also produces carbon monoxide, carbon dioxide and methane but acetate

* Corresponding author. Tel.: +34-965-903-867; fax: +34-965-903-826.
*E-mail address:* antonio.marcilla@us.es (A. Marcilla).

0032-3861/01/$ - see front matter 
PII: S0032-3861(01)00277-4

pyrolysis is the favoured reaction. A second reaction, at approximately 745 K, breaks the polyunsaturated hydrocarbon adjacent to the double bond. The saturated fragment may either add hydrogen to produce a terminal methyl group or lose hydrogen to produce a vinyl group. The first pathway seems to be favoured. Alternatively, the unsaturated terminal groups add hydrogen to produce a vinyl terminated fragment. Depending on what happens at the other end of the fragment on subsequent decomposition, either an alkane, or an alkene or a 1,*n*-diene is produced.

Several authors have studied the influence of different catalysts on the mechanism of thermal decomposition of different waste products as well as on the values of the corresponding kinetic parameters [12–17]. The addition of a catalyst could not only improve the quality of products obtained from pyrolysis of plastic wastes and lower the temperature of decomposition, but could also enable a given selectivity to a certain product to be achieved. The application of acid solids, such as zeolites and related materials, in the catalytic pyrolysis of polymers is relatively recent and the number of scientific papers published on this issue demonstrates its interest [17–27]. These catalysts favour hydrogen transfer reactions due to the presence of many acid centres [17]. Zeolites have a diffusion and molecular size porous nature with a fixed geometry which produces their relatively high reactivity as catalysts. The access of molecules to catalyst reactive sites, as well as the growth of end products inside the pores, is limited to the pore size [17]. Lin et al. [25] showed a summary of some important studies of catalytic pyrolysis of polymers using solid acid catalysts.

MCM-41 is a silica–alumina acid solid used as catalyst, being a crystalline material with a regular structure of hexagonal channels, whose diameter (and therefore its catalytic characteristics) can vary between 1.5 and 10 nm, depending on the synthesis conditions. This material has been studied for its potential application in the catalytic cracking of polyolefins [18–20,27,28].

Kinetic modelling is a powerful and sound technique of data reduction which is very valuable in the interpretation of the data from pyrolysis experiments. The advantages of this practice are obvious for engineering purposes and with modern computers, very good correlation of the experimental data can be achieved in negligible time. The kinetic parameters obtained allow the immediate reproduction of the data as well as interpolations. Especially in peak separation, this practice is very useful since it allows very objective results to be obtained, according to the model. Obviously, to develop a really mechanistic kinetic model, or being more ambitious the actual kinetic model, is almost an impossible task, since a large number of interacting processes (both physical and chemical) are always involved in this type of reaction and different complementary techniques must be used to obtain information about the different products and intermediates. Thus, if only the TG data are to be considered, and being realistic, pseudo-kinetic models can be developed. These models must be able to represent all the features observed and should remain as simple as possible. To fulfil these two requirements, a balance among the number of kinetic equations (and their corresponding number of parameters) and the processes involved must be found. It is evident that a TG curve involving a single weight loss process may be represented by one simple kinetic equation with few parameters. However, it is obvious that if this model with the same parameters cannot correlate experiments at different heating rate, the model is not adequate, and a more complex one must be developed. In the case of complex TG curves with more than one peak, the corresponding model should have different terms corresponding to the different processes, increasing accordingly the number of parameters.

Marcilla and Beltrán [6] tested two different kinetic models to explain the thermal decomposition of an EVA copolymer. Both kinetic models involved an intermediate species, and the second one allowed an alternative reaction. Marcilla et al. [28] have suggested a kinetic model for the MCM-41 catalytic decomposition of PE, where both the thermal and catalytic routes are allowed. The combination of these models may adequately correlate the weight loss curves of the EVA copolymers, both catalytic and thermal at different heating rates.

Therefore, the objective of the present work is to study by dynamic TG the thermal and MCM-41 catalytic pyrolysis of the EVA copolymer, and to develop and apply a kinetic model based on two previous models suggested for the thermal decomposition of EVA and the thermal and catalytic decomposition of PE. To test the model, six commercial EVA copolymers with different VA content and properties were pyrolysed at different heating rates, with and without the MCM-41 catalyst.

## 2. Equipment and experimental procedure

### 2.1. Thermobalance

The experiments were carried out in a Netzsch Thermobalance, model TG209 controlled by a PC under the Windows operating system. The atmosphere used was nitrogen (99.99% minimum purity) with a flow rate of 30 STP ml/min, according to the specifications of the equipment. The sample temperature was measured with a thermocouple directly at the crucible, i.e. very close to the sample.

### 2.2. Material and operating conditions

The experiments were carried out with six different samples of commercial EVA copolymers. The samples cover a wide range of vinyl percentage, hardness and melt flow indexes (MFIs). Table 1 shows the main characteristics of the polymers studied. The catalyst used was MCM-41 synthesized by the basic hydrothermal method [27,29].

Table 1
Characteristics of the six commercial EVA copolymers studied

| Commercial name of polymer | VA (%) | MFI[a] | Hardness | Notation |
|---|---|---|---|---|
| EVA BASF LUPOLEN V-3510-K | 13 | 4 | 84 | Sample 1 |
| EVA DUPONT (ELVAX) | 18 | 2.5 | 90 | Sample 2 |
| EVA ESCORENE UL15028CC | 27.5 | 145 | 69 | Sample 3 |
| EVA ESCORENE UL04533CC | 33 | 46 | 67 | Sample 4 |
| EVA ESCORENE UL05540CC | 39 | 60 | 55 | Sample 5 |
| EVA, 40% VA | 40 | 30 | – | Sample 6 |

[a] Melt flow index (g/10 min).

The main characteristics of this catalyst are summarized in Table 2. Experiments in dynamic conditions were carried out over a range of temperatures that included the entire range of solid decomposition, 450–875 K, with heating rates of 10 and 40 K/min. The experiments were replicated at least twice to determine their reproducibility. For example, Fig. 1 shows the curves obtained for Sample 1 at 10 and 40 K/min, and for Sample 1 with around 9% of MCM-41, at 10 K/min. As can be seen, the reproducibility is very good. The rest of experiments show similar reproducibility and a maximum deviation between the repeated pyrolysis runs of about 2% was observed.

The mass of the sample used ranged between 5 and 25 mg. The values of temperature considered were those recorded by the thermocouple situated below the sample and very close to it, and not those programmed.

A calibration procedure was performed using internal standards (alumel, nickel and perkalloy) in all experiments. In a first run, only the sample was placed in the sample holder, whereas in a second run, the weight loss of the sample with the three metals or alloys was recorded. In this case, a magnet surrounded the oven and sample. The standards lose their magnetic properties at 436, 627 and 869 K, respectively. In this way, a control of the temperatures was available in every experiment, thus assuring the reliability of the temperatures.

Table 2
Physico-chemical and structural properties of MCM-41 prepared by Escola [27]

| Property | Value |
|---|---|
| $d_{100}$, RX diffraction peak (nm) | 3.76 |
| $a_0$, unit cell dimensions (nm) | 4.34 |
| Pore size (nm) | 2.72 |
| Wall thickness (nm) | 1.62 |
| BET area ($m^2/g$) | 1357 |
| Total volume of pores ($P/P_0 = 0.995$, $cm^3/g$) | 1.51 |
| Volume of pores ($P/P_0 = 0.6$, $cm^3/g$) | 1.08 |
| Si/Al ratio | 42.7 |
| Acidity ($NH_3$ meq/g) | 0.30 |
| Temperature of the maximum of $NH_3$ desortion (°C) | 314 |

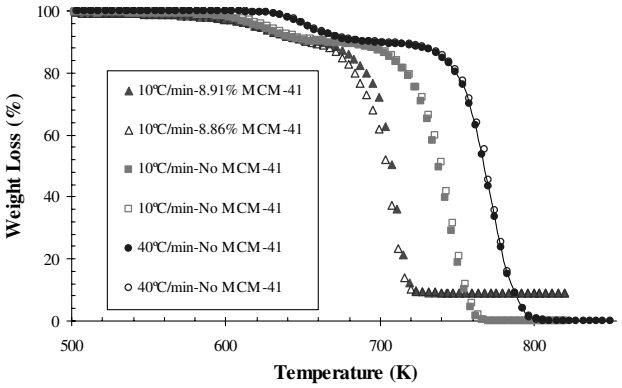


Fig. 1. Repeated TG curves for Sample 1 at two heating rates and for the thermal and catalytic processes.

## 3. Results and discussion

### 3.1. Thermal decomposition at different heating rates

Fig. 2a and b shows the TG curves at 10 and 40 K/min, respectively, for the six samples studied. As can be seen, at each heating rate, the two thermal decomposition processes occur at similar temperatures for all the samples, regardless of the amount of VA. Table 3 shows the corresponding peak temperatures for the first weight loss ($T_1$), corresponding to the elimination of the VA units from the polymer chains,

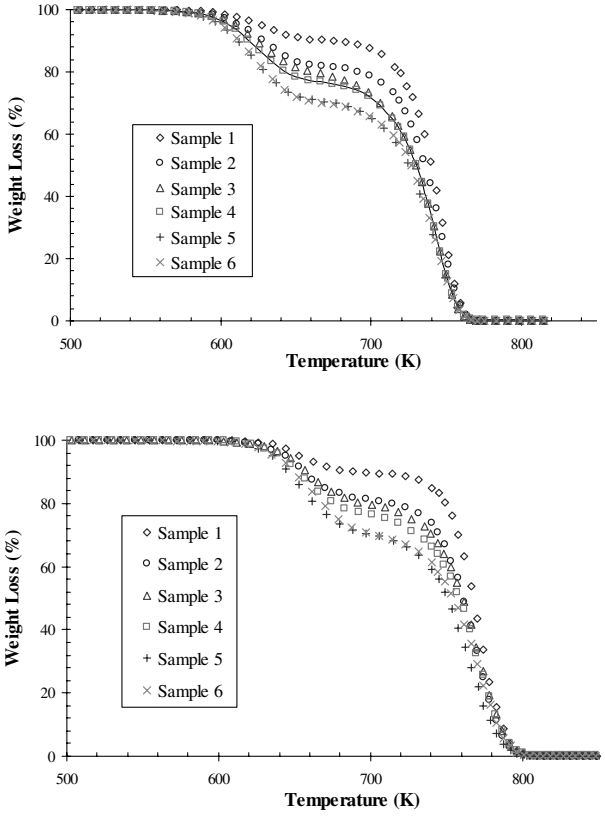


Fig. 2. TG curves for the six EVA copolymers studied at (a) 10 K/min and (b) 40 K/min.

Table 3
Characteristics of different TG runs performed

| EVA sample | Heating rate (K/min) | EVA mass (mg) | % of MCM-41 | $T_1$ (K) | $T_2$ (K) |
|---|---|---|---|---|---|
| Sample 1 | 40 | 20.53 | 0.00 | 655.8 | 772.5 |
| Sample 1 | 40 | 13.09 | 9.10 | 660.5 | 740.3 |
| Sample 1 | 10 | 5.88 | 0.00 | 627.1 | 746.9 |
| Sample 1 | 10 | 10.39 | 8.90 | 626.3 | 709.3 |
| Sample 2 | 40 | 18.72 | 0.00 | 648.8 | 770.1 |
| Sample 2 | 40 | 10.12 | 9.12 | 663.5 | 745.5 |
| Sample 2 | 10 | 7.17 | 0.00 | 629.2 | 746.4 |
| Sample 2 | 10 | 7.96 | 9.09 | 626.8 | 719.8 |
| Sample 3 | 40 | 16.30 | 0.00 | 664.0 | 774.2 |
| Sample 3 | 40 | 22.55 | 9.33 | 659.5 | 758.3 |
| Sample 3 | 10 | 4.99 | 0.00 | 630.7 | 744.4 |
| Sample 3 | 10 | 11.26 | 9.10 | 630.3 | 726.7 |
| Sample 4 | 40 | 19.10 | 0.00 | 655.8 | 770.1 |
| Sample 4 | 40 | 16.65 | 9.07 | 661.2 | 757.6 |
| Sample 4 | 10 | 4.63 | 0.00 | 626.3 | 744.0 |
| Sample 4 | 10 | 10.55 | 9.09 | 628.1 | 729.1 |
| Sample 5 | 40 | 23.71 | 0.00 | 656.7 | 764.6 |
| Sample 5 | 40 | 10.26 | 9.36 | 659.4 | 751.0 |
| Sample 5 | 10 | 6.55 | 0.00 | 624.1 | 742.4 |
| Sample 5 | 10 | 12.98 | 9.17 | 629.3 | 732.6 |
| Sample 6 | 40 | 15.33 | 0.00 | 658.7 | 771.8 |
| Sample 6 | 40 | 14.99 | 7.98 | 650.7 | 756.8 |
| Sample 6 | 10 | 5.53 | 0.00 | 623.3 | 743.2 |
| Sample 6 | 10 | 10.64 | 9.06 | 626.5 | 731.1 |

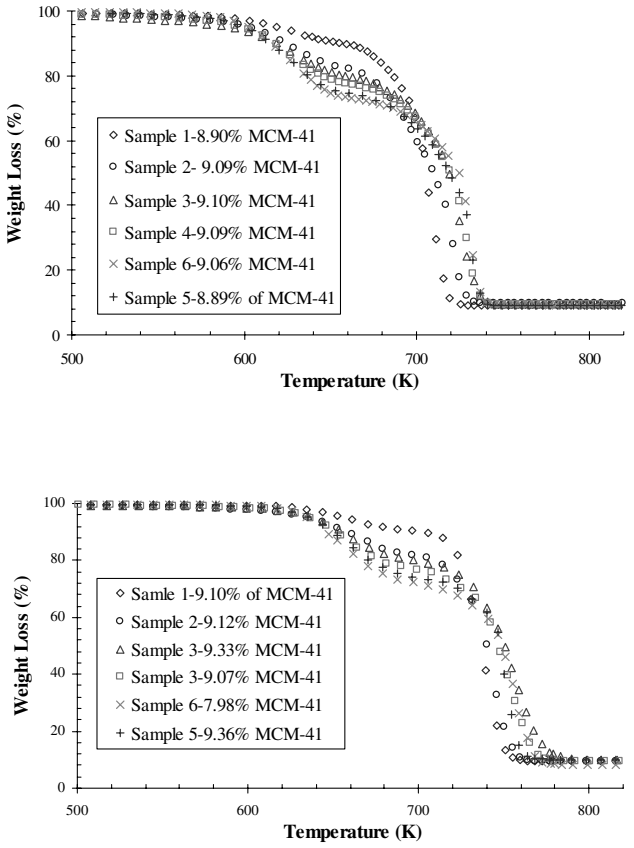


Fig. 3. TG curves for the catalytic pyrolysis of the six EVA copolymers studied with around 9% of MCM-41 at (a) 10 K/min and (b) 40 K/min.

and the peak temperature for the second weight loss ($T_2$), corresponding to the decomposition of the polyolefin chain resulting from the first process and of the polyethylene domains of the polymer. These results are in good agreement with those reported by other authors [6,9,10,30,31]. As can be expected for these types of processes, both thermal degradation temperatures, $T_1$ and $T_2$, increase when the heating rate increases but the first process presents a higher temperature shift than the second one. Also, the second thermal decomposition process occurs at temperatures very close to those of a polyethylene polymer, regardless of the VA content and the different properties of the samples studied.

### 3.2. Catalytic decomposition at different heating rates

Fig. 3a and b shows the results obtained for the six EVA samples with around 9% of MCM-41 acidic catalyst at 10 and 40°K/min, respectively. The corresponding characteristics for each TG run are shown in Table 3. The curves present similar trends as the thermal pyrograms, showing the shifting effect of the heating rate. In this case, the curves show a final residue corresponding to the weight of catalyst used. A closer inspection of these curves and a comparison with those corresponding to their thermal pyrolysis and the pyrolysis of PE, both thermal and catalytic, reveal very interesting features.

Figs. 4–9 show the TG curves corresponding to the six samples studied, both thermal and catalytic at two heating rates. The figures are ordered by increasing VA content. It can be observed that the catalytic process starts at lower temperatures than the thermal process, and progresses with a slow weight loss rate up to the temperature of the acetic acid evolution, around 620 K at 10 K/min and 650 K at 40 K/min. This behaviour is very similar to that observed for the PE. It seems that in the PE polymer and in the PE

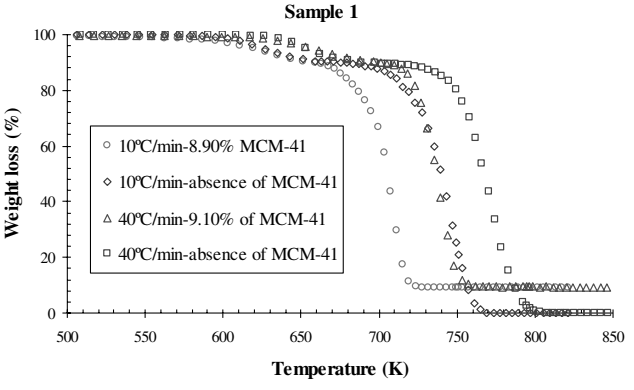


Fig. 4. Experimental TG curves obtained for Sample 1.

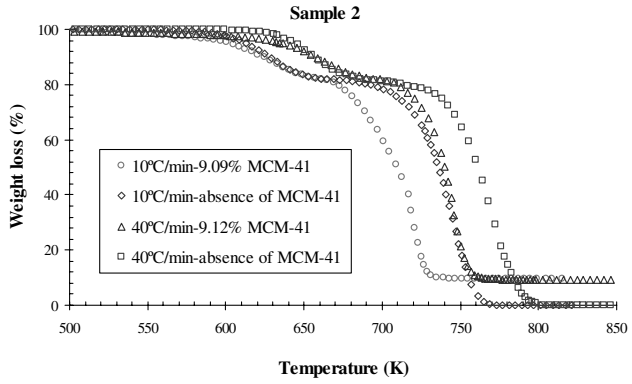


Fig. 5. Experimental TG curves obtained for Sample 2.

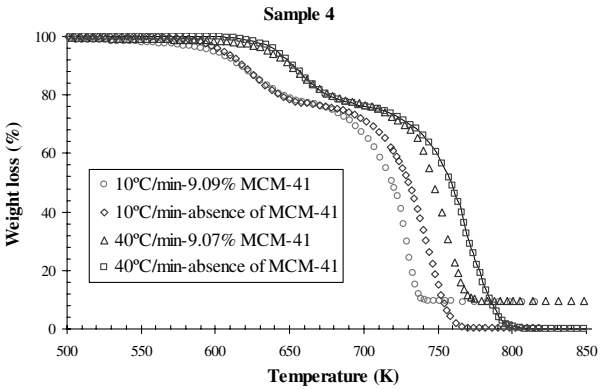


Fig. 7. Experimental TG curves obtained for Sample 4.

domains of the EVA copolymer, there are a sort of sites that interact with the catalyst at low temperatures producing an early thermal destabilization but with a low weight loss rate. The first main loss of weight, i.e. that corresponding to the VA elimination, suffers almost no modification and appears at the same temperature despite the presence of the catalyst. Contrarily, the second weight loss corresponding to the decomposition of the PE domains and of the polyene residue after the evolution of VA is clearly affected by the presence of the MCM-41 catalyst, and a shift to lower temperatures can be observed. This effect is more marked as the amount of VA in the copolymer decreases, i.e. the copolymer is more similar to a PE polymer.

Another feature that can be observed is that the increase in the weight loss rate in the case of the catalytic pyrolysis, due to the decomposition of the PE domains of the EVA, is produced at different temperatures depending on the VA content of the samples. In the case of Sample 1, with the lowest VA content, this effect is observed already from the plateau between the two main processes (VA evolution and PE decomposition) being the effect of the catalyst on the second process similar to those of the pure PE decomposition. However, on increasing the VA content in the samples, the second process shows two zones corresponding to the PE and polyene domains decomposition, showing also a lower decrease of the corresponding characteristic temperature.

Therefore, it seems as if the catalyst is only effective when accelerating the decomposition process of the PE domains but with a little effect on the VA domains as well as on the polyene residue after the acetic acid evolution. According to Ref. [17], the catalytic action is explained by the interaction of the ends of the chains and branches of the polymer with the active sites of the catalyst, which are affected by important steric effects. In the case of the acetic acid evolution, according to Munteanu and Turcu [10], a six-atom-ring transition state is required. This large intermediate species is not likely to enter the pore structure of the catalyst and consequently the catalyst does not alter this process. Furthermore, these authors indicated that the double bonds formed on the grafted chains have a '*trans*' configuration, which favours the cross-linking. It seems that these structures are also not affected by the presence of the catalyst, which mainly interacts with the PE domains of the copolymer.

### 3.3. Kinetic modelling

To explain the behaviour of the thermal and catalytic pyrolysis of EVA copolymers, a kinetic model has been proposed, based on the one applied by Marcilla and Beltrán [6] and by Marcilla et al. [28] assuming the following steps:

$$\mathrm{EVA} \xrightarrow{k_1} s\,\mathrm{EVA}^{*} + (1-s)\mathrm{G}_1 \qquad \text{(R1)}$$

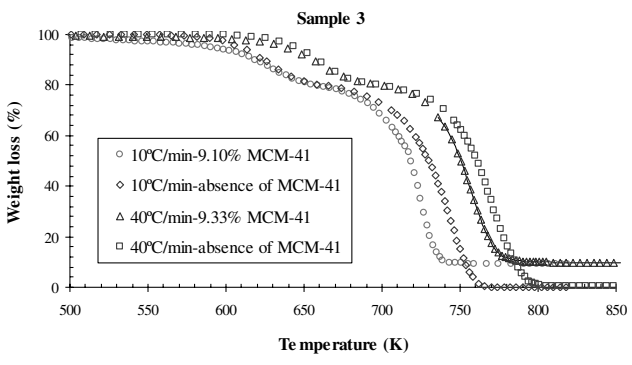


Fig. 6. Experimental TG curves obtained for Sample 3.

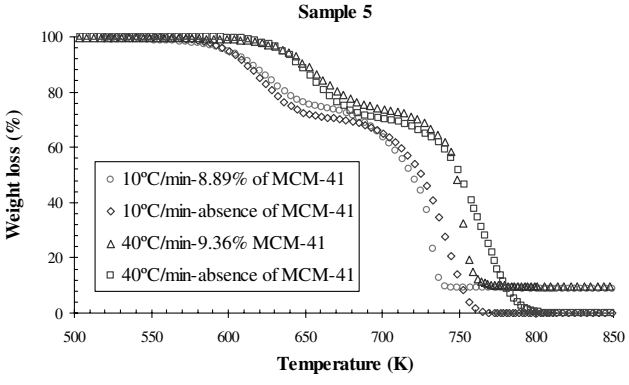


Fig. 8. Experimental TG curves obtained for Sample 5.

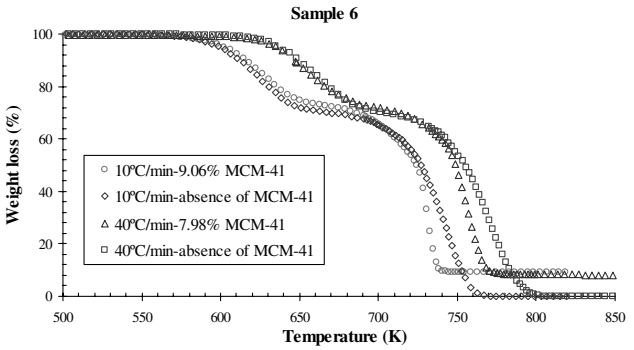


Fig. 9. Experimental TG curves obtained for Sample 6.

$$\mathrm{EVA}^{*} \xrightarrow{k_2} \mathrm{G}_2 \tag{R2}$$

$$\mathrm{EVA}^{*} + c\,\mathrm{C} \xrightarrow{k_v} (1+c)\mathrm{EVA}^{*}\mathrm{C} \xrightarrow{k_4} \mathrm{G}_3 + c\,\mathrm{C} \tag{R3}$$

where EVA is the initial EVA copolymer, $\mathrm{EVA}^{*}$ the intermediate formed by the acetic acid elimination, C the catalyst, $\mathrm{EVA}^{*}\mathrm{C}$ an intermediate in the catalytic reaction and $\mathrm{G}_1$, $\mathrm{G}_2$ and $\mathrm{G}_3$ the volatiles produced by the corresponding reactions (R1)–(R3), respectively. $s$ represents the yield coefficients for the first process and $c$ is related to the grams of free catalyst per gram of $\mathrm{EVA}^{*}$ intermediate necessary to obtain the complex $\mathrm{EVA}^{*}\mathrm{C}$. As the thermobalance does distinguish between the different solid species, the TG data can be used only to study the global weight-loss kinetics. The kinetic equations representing the scheme presented, if an $n$th order kinetics is considered, are

$$\frac{\mathrm{dEVA}}{\mathrm{d}t} = -k_1\mathrm{EVA}^{n_1} \tag{1}$$

$$\frac{\mathrm{dEVA}^{*}}{\mathrm{d}t} = sk_1\mathrm{EVA}^{n_1} - k_2\mathrm{EVA}^{*n_2} - k_v\mathrm{EVA}^{*n_3}\mathrm{C}^{n_4} \tag{2}$$

$$\frac{\mathrm{dC}}{\mathrm{d}t} = -ck_v\mathrm{EVA}^{*n_3}\mathrm{C}^{n_4} + ck_4\mathrm{EVA}^{*}\mathrm{C}^{n_5} \tag{3}$$

$$\frac{\mathrm{dEVA}^{*}\mathrm{C}}{\mathrm{d}t} = (1+c)k_v\mathrm{EVA}^{*n_3}\mathrm{C}^{n_4} - (1+c)k_4\mathrm{EVA}^{*}\mathrm{C}^{n_5} \tag{4}$$

$$\frac{\mathrm{dG}_1}{\mathrm{d}t} = (1-s)k_1\mathrm{EVA}^{n_1} \tag{5}$$

$$\frac{\mathrm{dG}_2}{\mathrm{d}t} = k_2\mathrm{EVA}^{*n_2} \tag{6}$$

$$\frac{\mathrm{dG}_3}{\mathrm{d}t} = k_4\mathrm{EVA}^{*}\mathrm{C}^{n_5} \tag{7}$$

where $n_1$, $n_2$, $n_3$, $n_4$ and $n_5$ are the reaction orders. The rate constants $k_1$, $k_2$, $k_3$ and $k_4$ can be expressed by the Arrhenius law:

$$k_i = k_{0,i}\exp\left(\frac{-E_i}{RT}\right) = k_{0\mathrm{ref},i}\exp\left[-\frac{E_i}{R}\left(\frac{1}{T} - \frac{1}{T_{\mathrm{ref}}}\right)\right] \tag{8}$$

$T_{\mathrm{ref}}$ is a temperature within the range of significant weight loss rate (650 K in this case) that is used to scale and diminish the interrelation among the parameters and help the optimisation search [32].

According to Marcilla et al. [28], the kinetic constant $k_v$ in scheme (R2) has been modelled with the following equation:

$$k_v = \frac{k_3\mathrm{C}_0}{K_{\mathrm{F}} + \mathrm{C}_0} \tag{9}$$

where $\mathrm{C}_0$ represents the initial amount of catalyst and $K_{\mathrm{F}}$ is a constant.

Bearing in mind that the weight measured is the addition of all the solid species present, it can be written that

$$\frac{\mathrm{d}w}{\mathrm{d}t} = \frac{\mathrm{dEVA}}{\mathrm{d}t} + \frac{\mathrm{dEVA}^{*}}{\mathrm{d}t} + \frac{\mathrm{dC}}{\mathrm{d}t} + \frac{\mathrm{dEVA}^{*}\mathrm{C}}{\mathrm{d}t} = -\frac{\mathrm{dG}_1}{\mathrm{d}t} - \frac{\mathrm{dG}_2}{\mathrm{d}t} - \frac{\mathrm{dG}_3}{\mathrm{d}t} \tag{10}$$

Taking into account Eqs. (5)–(7), we have

$$\frac{\mathrm{d}w}{\mathrm{d}t} = (s-1)k_1(\mathrm{EVA})^{n_1} - k_2(\mathrm{EVA}^{*})^{n_2} - k_4(\mathrm{EVA}^{*}\mathrm{C})^{n_5} \tag{11}$$

The initial boundary condition for this differential equation is, obviously, $w = \mathrm{EVA} + \mathrm{C} = 1$ and $\mathrm{EVA}^{*} = \mathrm{EVA}^{*}\mathrm{C} = 0$ when $t = 0$ The parameter $c$ has very little influence on the fitting and exactly the same results (both quality of the correlation and value of the rest of the parameters) are obtained for values below 0.1. Thus, the correlation has been carried out fixing this parameter at 0.001.

The models developed in the present work have been applied to correlate simultaneously the TG and DTG curves obtained under dynamic conditions at heating rates of 10 and 40 K/min, trying to better reproduce the details of all the curves. In all the calculations, the objective function (O.F.) included the TG and DTG data obtained at all the heating rates for the same EVA with and without the catalyst:

$$\mathrm{O.F.} = \sum_{j=1}^{2}\sum_{m=1}^{M}\left\{((w_{m,j})_{\mathrm{exp}} - (w_{m,j})_{\mathrm{cal}})^2 + 10\left[\left(\frac{\mathrm{d}(w_{m,j})}{\mathrm{d}T}\right)_{\mathrm{exp}} - \left(\frac{\mathrm{d}(w_{m,j})}{\mathrm{d}T}\right)_{\mathrm{cal}}\right]^2\right\} \tag{12}$$

where $m$ represents the experimental (exp) or calculated (cal) data at temperature $T_{\mathrm{m}}$ and time $t_{\mathrm{m}}$ of the experiment at heating rate $j$ and $M$ the number of experimental points. $w$ is the weight fraction, this means the weight at the time $t$ divided by the initial weight of the sample. The kinetic parameters were optimised using the tool 'Solver' included in the calculation sheet Excel 7.0 for Windows. The integration of the kinetic equations was carried out using the Euler method.

The application of the previous model, considering

simultaneously the four TG and DTG curves obtained for each sample showed that, systematically, the curves corresponding to the experiments with higher initial mass sample were worse fitted. According to the literature, i.e. [33–35], this effect can be attributed to differences between the actual and nominal temperature. For this reason, several authors have considered this effect on their kinetic models. For instance, in a previous work [33], we introduced the energy balance in order to correct the temperature and a more complicated model was developed. In this case, and since the model is already more complex and due to the difficulty in knowing exactly the term corresponding to the apparatus response in the energy balance, we have adopted another approach that involves the following assumptions:

$$T_j = T_{j,\mathrm{exp}} + \alpha_i w_{\mathrm{cal}} \tag{13}$$

indicating that the 'actual' temperature ($T_j$) at the time $t_j$ differs from the nominal one ($T_{j,\mathrm{exp}}$) proportionally to the mass present in the sample holder. In this way, this parameter takes into account in a very simple and effective way the influence of the initial mass of sample. More sophisticated corrections can be devised but the improvement in the fitting is negligible (if positive) compared with this approximation. $\alpha_i$ is a parameter in the experiment $i$ that depends on the initial mass as follows:

$$\alpha_i = \frac{\alpha_0 W_{0i}}{\max(W_{0i})} \tag{14}$$

where $W_{0i}$ represents the initial mass of EVA copolymer and catalyst in experiment $i$. Within each series of experiment with the same EVA copolymer, $\alpha_0$ is the only additional adjustable parameter introduced which takes into account all the factors affecting the actual temperature.

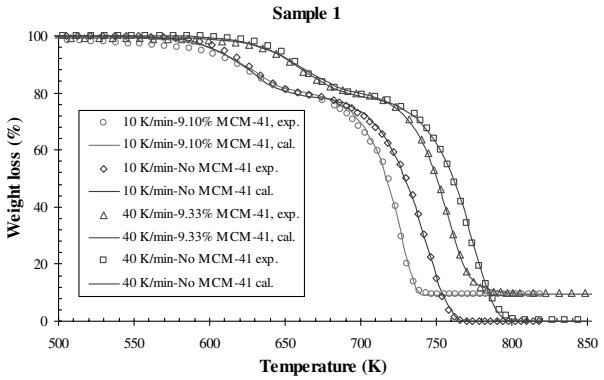


Fig. 10. Comparison between the experimental and calculated TG curves for Sample 3.

Considering the Arrhenius type behaviour of the rate constants, the number of parameters is $4 \times k_{i0}$, $4 \times (E_i/R)$, $5 \times n_i$, $K_{\mathrm{F}}$ and the coefficients $s$ and $\alpha_0$, i.e. a total of 16. This number of parameters can be considered not excessive if bearing in mind that experiments involving two main peaks in the DTG curve, at different heating rates, with and without catalyst and with significantly different initial mass are simultaneously correlated.

### 3.4. Kinetic model results

Table 4 shows the parameters obtained and the O.F. values for the six samples studied. As can be seen, the proposed model satisfactorily fits the different decomposition processes, especially when considering that all the experiments (at different heating rate, with different catalyst content and with different initial sample weight) are correlated simultaneously. For example, Fig. 10 shows the

Table 4
Kinetic parameters for the six EVA samples studied

| Parameter | Sample 1 | Sample 2 | Sample 3 | Sample 4 | Sample 5 | Sample 6 |
|---|---|---|---|---|---|---|
| $s$ | 0.90 | 0.82 | 0.79 | 0.77 | 0.70 | 0.70 |
| $k_{01,\mathrm{ref}}$ ($\mathrm{min}^{-1}$) | 3.765 | 2.322 | 1.959 | 1.471 | 2.032 | 1.962 |
| $E_1/R$ ($\mathrm{K}^{-1}$) | 23 384 | 21 336 | 19 498 | 19 077 | 20 385 | 19 187 |
| $n_1$ | 1.29 | 1.22 | 1.18 | 0.90 | 1.32 | 1.13 |
| $k_{02,\mathrm{ref}}$ ($\mathrm{min}^{-1}$) | 0.0006 | 0.0009 | 0.0026 | 0.0021 | 0.0018 | 0.0021 |
| $E_2/R$ ($\mathrm{K}^{-1}$) | 36 551 | 34 134 | 28 247 | 28 832 | 32 102 | 30 535 |
| $n_2$ | 1.14 | 1.04 | 0.91 | 0.84 | 1.11 | 1.06 |
| $k_{03,\mathrm{ref}}$ ($\mathrm{min}^{-1}$) | 1.661 | 18.101 | 0.270 | 1.757 | 0.781 | 0.700 |
| $E_3/R$ ($\mathrm{K}^{-1}$) | 36 191 | 28 267 | 31 520 | 31 474 | 45 234 | 12 235 |
| $n_3$ | 0.57 | 0.46 | 0.40 | 0.31 | 0.30 | 0.36 |
| $n_4$ | 1.92 | 2.89 | 1.76 | 2.67 | 3.11 | 0.72 |
| $K_{\mathrm{F}}$ | 0.065 | 0.119 | 0.059 | 0.058 | 0.065 | 0.106 |
| $k_{04,\mathrm{ref}}$ ($\mathrm{min}^{-1}$) | 2.111 | 309.5 | 3.496 | 3.682 | 0.060 | 0.001 |
| $E_4/R$ ($\mathrm{K}^{-1}$) | 8590 | 2317 | 1025 | 1037 | 26 145 | 37 361 |
| $n_5$ | 1.28 | 2.18 | 1.06 | 0.94 | 1.32 | 0.42 |
| $\alpha_0$ | −17.4 | −11.4 | −19.9 | −7.6 | −11.3 | −18.1 |
| FO | 0.040 | 0.072 | 0.051 | 0.062 | 0.082 | 0.050 |

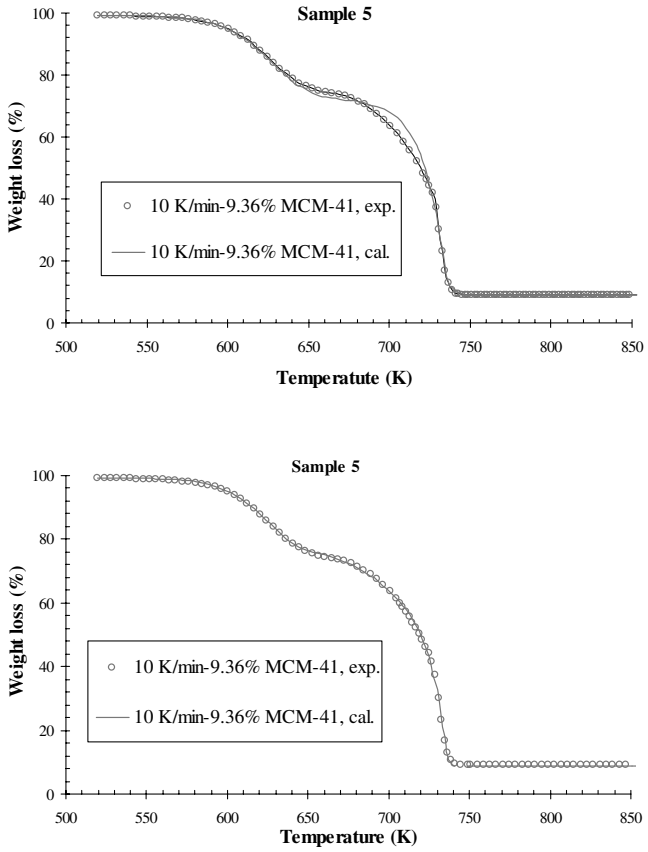


Fig. 11. Comparison between the fit obtained for Sample 5, at 10 K, when the four curves have been considered simultaneously and when only one TG curve has been fitted.

experimental and calculated TG curves for Sample 3, which is representative of the rest of the EVA copolymers studied.

Comparing the experimental and calculated TG curves corresponding to the catalytic pyrolysis, small differences can be observed. These differences could be attributed to the actual data dispersion or to the incapability of the proposed kinetic model to explain the behaviour observed qualitatively. However, when the proposed kinetic model is applied to only one experiment it can seen that the model can actually correlate the whole behaviour of the TG curve perfectly, i.e. the beginning of the catalyst reaction at low temperatures, the VA evolution and the different decomposition of PE and polyene domains. For example, Fig. 11 shows the calculated TG curve for the catalyst pyrolysis of Sample 5 with a heating rate of 10 K/min using all four TG experiment (at different heating rates, with different catalyst content and with different initial sample weight), and using only the corresponding experimental curve at 10 K/min. From these results, it is evident that the proposed model can provide an adequate representation of the processes involved, and that the deviations due to the dispersion of the experimental data in a single TG run, enhanced by the fact of simultaneously fitting experiments at different heating rate, with different catalyst content and with different initial sample weight, must be responsible for the observed average results. Obviously, it is also possible to observe a clear correlation between the parameter $s$ related with the fraction of the initial copolymer that remains after the elimination of the VA, i.e. with the VA content of the copolymer.

The values of the kinetic parameters shown in Table 4 are in agreement with those found in literature for reactions (R1) and (R2) with reaction orders for the EVA and EVA$^*$ close to 1 [6] and activation energy for (R2) higher than for (R1), with an $E_1/R$ between 19 600 and 22 400 $K^{-1}$ and an $E_2/R$ between 29 900 and 32 500 $K^{-1}$ in good agreement with other authors [30,31].

## 4. Conclusions

The study of the TG curves corresponding to the thermal and catalytic decomposition of EVA copolymers studied shows that the catalyst seems only to affect the PE domains in the copolymer, whereas the acetic acid loss is practically independent of the presence of the catalyst. The presence of MCM-41 as a catalyst produces a decrease in the thermal temperature decomposition for the second process in the degradation of EVA copolymers. This process seems to be similar to the PE catalytic decomposition, and the similarity decreases when the VA contents increase.

The dynamic kinetics of the catalytic pyrolysis can be satisfactorily modelled assuming two independent processes and the catalyst action of the MCM-41 on the residue after the VA evolution and the PE domains of the copolymer using kinetic parameters independent of the heating rate. The model is capable of reproducing or correlating all the details observed in a single TG, whereas the correlation is logically smoothed when simultaneously fitting all experiments corresponding to a given EVA copolymer.

## Acknowledgements

The authors are grateful to the Department of Chemical Engineering of the University Complutense of Madrid (Spain) for supplying the MCM41 catalyst. Financial support for this investigation has been provided by the Spanish 'Comisión de Investigación Científica y Tecnológica' de la Secretaría de Estado de Educación, Universidades, Investigación y Desarrollo (CICYT PB96-0329).

## References

[1] Odian G. Principles of polymerization. 3rd ed. New York: Wiley, 1991.
[2] Brandup J. Macromol Symp 1998;135:223–35.
[3] Verdú E, Devesa J, Maldonado F, Porta E. Revista Plást Mod 1988;390:893–8.
[4] Washall JW, Wampler TP. Spectroscopy 1990;6(4):38–42.
[5] McGrattan BJ. Appl Spectr 1993;48(12):1472–6.
[6] Marcilla M, Beltrán M. Polym Degrad Stab 1995;50:117–24.

[7] Häußler L, Pompe G, Albrecht V, Voigt D. J Thermoanal 1998;52:131–43.
[8] Marcilla A, Reyes JA, Sempere FJ. Polymer 2001;42(12):5343–50.
[9] Munteanu D, Turcu S. Mater Plast 1977;14:144.
[10] Munteanu D, Turcu S. J Therm Anal 1981;20:281.
[11] Moskala EJ, Lee DW. Polym Degrad Stab 1989;25:11.
[12] Varhegyi G, Antal MJ. Energy Fuels 1988;2:267–72.
[13] Caballero JA, Font R, Marcilla A, Conesa J. Ind Engng Chem Res 1995;34:806–12.
[14] Ohkita H, Nishiyama R, Tochihara Y, Mizushima T, Kakuta N, Morioka Y, Ueno A, Namiki Y, Tanifuji S, Katoh H, Sunazuka H, Nakayama R, Kuroyanagi T. Ind Engng Chem Res 1993;32:3112–6.
[15] Blazsó M. J Anal Appl Pyrol 1999;49:125–43.
[16] Blazsó M. J Anal Appl Pyrol 1999;51:73–78.
[17] Pinto F, Costa P, Gulyurtlu I, Cabrita I. J Anal Appl Pyrol 1999;51:57–71.
[18] Mordi RC, Fields R, Dwyer J. J Chem Soc, Chem Commun 1992:374–5.
[19] Aguado J, Serrano DP, Romero MD, Escola JM. Chem Commun 1995;1:725.
[20] Serrano DP, Aguado J, Sotelo JL, Van Grieken R, Escola JM, Menéndez JM. Stud Surf Sci Catal 1998;117:437–44.
[21] Uemichi Y, Kashwaya Y, Tsukidate M, Ayame A, Kanoh H. Bull Chem Soc Jpn 1983;56(9):2768–73.
[22] Sakata Y, Uddin A, Koizumi A, Murata K. Chem Lett, Chem Soc Jpn 1996:245–6.
[23] Sakata Y, Uddin A, Muto A. J Anal Appl Pyrol 1999;51:135–55.
[24] Uemichi Y, Takuma K, Ayame A. Chem Commun 1998:1975–6.
[25] Lin YH, Sharratt PN, Garforth, Dwyer J. Thermochim Acta 1997;294:45–50.
[26] Olazar M, Aguado R, Bilbao J, Barona A. AIChE J 2000;46(5):1025–33.
[27] Escola Sáez JM. PhD Thesis. Madrid: Universidad Complutense de Madrid; 1998.
[28] Marcilla A, Beltrán M, Conesa JA. J Anal Appl Pyrol, 2001;58–59:117–26.
[29] Aguado J, Serrano DP, Escola JM. Micropor Mesopor Mater 2000;34:43–54.
[30] Day M, Cooney JD, Wiles DM. Polym Engng Sci 1989;29:19.
[31] Nam JD, Seferis JC. J Polym Sci, Polym Phys Ed 1991;29:601.
[32] Himmelblau DM. Process analysis statistical methods. New York: Wiley, 1968.
[33] Conesa JA, Marcilla A, Font R, Caballero JA. J Anal Appl Pyrol 1996;36:1–15.
[34] Bockhorn H, Hornung A, Hornung U. J Anal Appl Pyrol 1999;49:53–74.
[35] Bockhorn H, Hornung A, Hornung U. J Anal Appl Pyrol 1999;50:77–101.